https://dx.doi.org/10.4314/ijs.v26i1.3

KINETICS OF ANTIBACTERIAL ACTIVITIES OF CELLULOSE NANOCRYSTALS AND THEIR SILVER-ZINC OXIDE NANOCOMPOSITES: APPLICATION AS POTENTIAL DISINFECTANTS

Agunbiade, F. O.[1,*], Allen, E. E.[1] and Oyetibo, G. O.[2]

[1]Department of Chemistry, Faculty of Science, University of Lagos, Akoka, Lagos, Nigeria.
[2]Department of Microbiology, Faculty of Science, University of Lagos, Akoka, Lagos, Nigeria.
[*]Corresponding Author's Email: fagunbiade@unilag.edu.ng
(Received: 12th November, 2023; Accepted: 22nd March, 2024)

ABSTRACT

Cellulose nanocrystals (CNCs) were produced from corncob and used as reducing agent in the formation of ZnO/CNCs, Ag/CNCs, and ZnO-Ag/CNCs composites and applied as antibacterial agents for both gram-positive and gram-negative bacteria and the kinetics of microbial growth inhibition studied. The CNCs and composites were characterized by UV-visible and Fourier transform-infrared (FTIR) spectroscopy. The characterization results revealed that the functional groups of CNCs were affected by their interactions with Ag^{+} and Zn^{2+} ions. The composites at 100 mg/mL displayed activities against Gram-positive bacteria - *Bacillus subtilis, Staphylococcus aureus, Staphylococcus epidermis, Bacillus coagulans and Enterococcus faecalis* and Gram-negative bacteria - *Escherichia coli, Klebsiella pneumonia, Salmonella typhimurium, Pseudomonas aeruginosa, Enterococcus faecium and Acinetobacter baumanii*) bacteria with inhibitory zones ranged between 9-46 mm. The kinetics of inhibition showed that the composites treated water had 4 to 28 times lower rate constants compared to the untreated water. This implied that the composites inhibit growth rates and have the potential of disinfecting for between 4 to 28 h depending on the bacteria. The materials showed better growth inhibition rate on gram-positive bacteria than on gram-negative. These composites may have potential applications as disinfectants in personal care products and serve as more eco-friendly alternative disinfectants to chlorophenols.

Keywords: Cellulose nanocrystals, Antibacterial, Disinfection, Metal nanoparticles, Inhibition kinetics.

Abbreviations

CNCs	Cellulose Nanocrystals
NPs	Nanoparticles
UV-Vis	Ultraviolet- Visible
Ag/CNCs	Silver-cellulose nanocrystal
ZnO/CNCs	Zinc oxide-cellulose nanocrystals
ZnO-Ag/CNCs	Zinc oxide-silver-cellulose nanocrystals
FTIR	Fourier Transformed Infrared
LPS	Lipopolysaccharide

INTRODUCTION

In recent times, management of agricultural wastes such as orange mesocarp, sugarcane bagasse, almond seed husk, beans husk, corn cob among others have been lots of problems due to inadequate knowledge of converting these agricultural wastes to beneficial products (Azubuike *et al.*, 2011). It was reported in China alone that 28.9 million tons of agricultural wastes were generated and only about 5.7 % of the agricultural wastes were recycled while the remaining 94.3 % were either burnt off or discarded into landfill, thus creating environment challenges (Marsh and Bugusu, 2007). These agricultural wastes are biodegradable polymers and can be applied in various value added products such packaging materials, medical devices among others (Rasato, 2009; Chaudhary *et al.*, 2023). There are a number of factors such as poor mechanical properties, water sensitivity (Debeaufort *et al.*, 1998; Zhou and Xanthos, 2009) that are limiting their industrial applications. Others include; high gas permeability (Koh *et al.*, 2008) , and low heat distortion temperature (Ray and Bousmina, 2005). There are therefore ongoing research studies towards improving and/or controlling the properties of these polymers and enhance their applicability. Researchers have applied several methods such as chemical or mechanical exfoliation, thermal treatments for nanosizing these biomasses, or chain extending, blending or copolymerization to enhance the properties and usefulness of these biopolymers (Kylma *et al.*, 2001; Sarkar *et al.*, 2021; Zhou *et al.*, 2023).

There are increasing research efforts to investigate Cellulose nanocrystal (CNC) as an emerging renewable biopolymer material that can be potentially nano-sized for various applications

(Kvien *et al*, 2005; Mali and Sherje, 2022), particularly within the biopolymer matrices. CNCs are considered nanomaterial because of their characteristic rod-like fibre with 2 to 20 nanometers diameter, tens to hundreds of nanometers length nanocrystals sizes. They are extracted with chemical exfoliation after acid hydrolysis of cellulose (Habibi *et al*., 2010; Mali and Sherje, 2022). The conversion of cellulose biomass to CNCs confer on them good solubility in water, excellent mechanical properties increased adsorption capacity for guest molecules and cations (Xu *et al*., 2013; Yu *et al*., 2013). Application of CNCs as composites with other nanoparticles is an emerging area of research. Recent research works are being carried out on polymer composites or nanocomposites and their application as new materials made from polymers (e.g. cellulose nano-crystals) and nano-scale metals or metal nanoparticles (e.g. Ag nanoparticles, ZnO nanoparticles etc) (Alexandre and Dubois, 2000; Sorrentino *et al*., 2007; Gorrasi *et al*., 2008; Peponi *et al*., 2009). Moreover, the improved application of CNCs through polymer-metal nanocompositing with by the homogeneous distribution of nano-scale metals like Ag, Cu and Zn nanoparticle (NPs) in the polymer matrices, grant the products ability to reinforce the articles made from it. The metal nanoparticles posses better functional properties. Their mechanical, optical, conductivity, and thermal properties are significantly enhanced. They posses antimicrobial activities and are useful in various fields such as medical applications; automotive industry; magnetic and optical devices production; higher performance electronic; packaging industry etc. due to these enhancements (Chae *et al*., 2005; Armentano *et al*., 2009; Bianco *et al*., 2009; Raman *et al*., 2011).

Inorganic nanoparticles (INPs) have been successfully composited with polymer materials with resultant new properties exhibited by the host polymer materials. However, the synthesis of these polymer embedded INPs without aggregation during their incorporation is still a challenge because the aggregates formed will significantly decrease inorganic nanoparticles applicability. Synthesis of INPs is often by precipitation from their salt solution or reduction of their metal ions using capping agents to stop their aggregation into bulk materials. Mostly used capping agents like surfactants and polymeric ligands are prepared from non-renewable petrochemicals which necessitated sourcing for renewable biodegradable alternatives like CNCs. Thus, cellulose-base materials are now being used as capping agents, stabilizers, and carriers in synthesising INPs polymer nanocomposites (Shinsuke *et al*., 2009; Padalkar *et al*., 2010; Zhou *et al*., 2023). Zinc oxide nanoparticles (ZnO-NPs) is one of the INPs that is increasing of interest, being investigated for use to produce functional devices, catalysts, pigments, optical materials, cosmetics, UV-absorbers and additive in many industrial products (Kimn *et al*., 2012). Wang *et al*. (2012), documented the antibacterial activity of ZnO-NPs of sizes less than 100 nm. The application of ZnO-NPs as viable solution to stop infectious diseases due to its good antibacterial properties have been advocated for considerations (Stoimenov *et al*., 2002). In the last decade, silver nanoparticles (Ag-NPs) have been the focus of extensively research studies. It has been documented that Ag-NPs exhibit antioxidant and antibacterial properties (Lateef *et al*., 2016; Olabemiwo *et al*., 2020). These antioxidant and antibacterial activities of Ag-NPs have led to the development of diverse nano-sized silver products, such as surgical instruments, contraceptive and sterilisation devices, nano-sized silver-coated wound dressings among others (You *et al*., 2012). The strong motivations for the development and use of nanocomposites of Ag and ZnO for antibacterial purposes are the economical and efficient considerations because Ag is very expensive. Additionally, Chen *et al*. (2011) documented that materials of ZnO doped silver (ZnO/Ag) reduced the ionization energy of acceptors in ZnO thereby enhancing the emission of electrons that can induce antibacterial properties. Thus, Ag ions may produce effects that will enhance the antibacterial activity of ZnO. There is however paucity of information on their activities as nanocomposites with CNC and in particular the role of CNC/ZnO/Ag composite as antibacterial agents and the kinetics of their inhibitory activities has not been reported.

The studies and applications of ZnO-Ag heterostructure nanoparticles have received considerable attention, partly because different

nano-sized ZnO-NPs have been easily made through various simple processes and also because of the excellent chemical and physical properties Ag nanoparticles. Nano-sized ZnO is a bactericide and inhibits activities against both Gram-positive and Gram-negative bacteria (Karunakaran *et al.*, 2010). Therefore, the use of CNCs as a new stabilizer for the synthesis of ZnO-Ag/CNCs heterostructure NPs can prevent the formation of aggregated ZnO-Ag heterostructure, improve the stability of the nanoparticle dispersion, enhance the antibacterial properties, thermal and mechanical properties, which make it of more potential usefulness in the fields of biomedicine and as good antibacterial and multifunctional filler (Hong *et al.*, 2006; Azizi *et al.*, 2013). The application of CNC as capping agent is justified by its prevalence; its renewability; its many hydroxyl groups on its surface which can interact with metallic ion as against other capping agents currently being explored. Thus, to address the limited information in literature on the biosynthesis of bimetallic nanoparticles as against monometallic nanoparticles, ZnO-Ag/CNCs bimetallic nanoparticles were synthesized in this study to investigate their antibacterial properties due to the expected synergistic effects between the two elements. The need to extend knowledge on the rate (kinetics) of the bacterial inhibitory activities of ZnO-Ag/CNCs composite was also underscored in this study. Hence, in this work, we present the biosynthesis protocols for generating antibacterial biogenic ZnO-Ag composites on cellulose nanocrystals and studied the kinetics of its actions in inhibiting bacterial growth.

EXPERIMENTAL

Materials

The corn cobs were obtained from Badagry, Lagos State. They were all washed, dried and milled. Chemicals used include sodium hydroxide (NaOH), sodium hypochlorite (NaOCl), sulphuric acid (H_2SO_4), zinc acetate dihydrate ($Zn(CH_3CO_2)_2.2H_2O$), ethanol (CH_3CH_2OH), sodium periodate ($NaIO_4$), silver nitrate ($AgNO_3$), ammonium hydroxide (NH_4OH), barium chloride monohydrate ($BaCl_2H_2O$), Muller- Hinton Agar (MHA), Nutrient Broth (NB), Antibiotic Disks and ethylene glycol. All reagents were of analytical grade.

Standard cultures for antibacterial assays were procured from Microbiology Laboratory, University of Lagos, Nigeria. These include Gram-negative (*Escherichia coli*, *ATCC11229*, *Klebsiella pneumonia*, *BAA1705*, *Salmonella typhimurium*, *ATCC13311*, *Pseudomonas aeruginosa*, *ATCC15442*, *Enterococcus faecium*, *ATCC700221*, *Acinetobacter baumanii,MS01289518-1*) and Gram-positive (*Staphylococcus aureus, ATCC2600*, *S. aureus, 700699*, *S. aureus*, *71MRSA, S. epidermis, ATCC12228*, *Bacillus coagulans, UL02*, *Bacillus subtilis, UL01*, *Enterococcus faecalis, ATCC19433, E. faecalis*, *ATCC19437*) bacterial pathogens.

Synthesis Methods

Preparation of Cellulose Nanocrystals (CNCs)

Cellulose powder (α-cellulose) was isolated from corn cob by washing, cutting into pieces, oven-drying at 65 °C and pulverizing. 500 g of the pulverized corn cob was weighed, digested with 2 % w/v sodium hydroxide, at 100 °C for 3 h with constant stirring. Alpha cellulose was extracted using 2 L of 12 % w/v sodium hydroxide at 80 °C for 1 h. The extracted alpha cellulose was washed and filtered severally with distilled water until pH 7 and bleached with 1.3 L of 10 % w/v of sodium hypochlorite at room temperature. The CNCs was then obtained from the α-cellulose by subjecting it to chemical exfoliation with 50 % sulphuric acid for 1 h 30 min at room temperature after which the reaction mixture was further shaken using a shaker for 2 h. The product obtained after the 2 h of shaking was then repeatedly washed to a pH of 7, bleached and dried.

Preparation of ZnO/Cellulose Nanocrystals (ZnO/CNCs) Composites

Zinc oxide/cellulose nanocrystals composites were synthesized using the method reported by Azizi *et al.*, (2013a) and Azizi *et al.*, (2013b) with slight modifications. The CNCs was suspended in deionized water, zinc acetate dihydrate - $Zn(CH_3CO_2)_2.2H_2O$ - in ethanol (50 mL, 10 wt %) was added to it and stirred with magnetic stirrer. The weight ratio of $Zn(CH_3CO_2)_2.2H_2O$ and CNCs was 1:2. ZnO was precipitated on the CNC from the mixture with the dropwise addition of sodium hydroxide solution (100 mL, 5.0 M) and gentle stirring at 80 °C. The obtained product

(ZnO/CNCs composite) was separated by centrifugation and was then washed with distilled water and dried for 1 h at 120 °C for a complete transformation of the remaining zinc hydroxide to zinc oxide.

Preparation of Ag Nanoparticles/Cellulose Nanocrystals (Ag/CNCs) Composites

Ag/CNCs composite was synthesized with aqueous solution of 0.5 M $NaIO_4$ (4 mL) added to 1 mg/mL of cellulose nanocrystal suspension (25 mL) in distilled water. This was stirred for 6 h at room temperature after which 1 mL of ethylene glycol was added for the removal of excess sodium periodate and washed with distilled water based on the modified method of Drogat *et al.* (2011). The reaction was completed by mixing together 5 mL of 5 mM $AgNO_3$ and 0.5 mL of 37 % NH_4OH and added to the oxidized cellulose nanocrystals. The reaction was stirred with magnetic stirrer at 50 °C for 30 min until brown suspension was formed which was stored in the dark at 4 °C prior to characterization and application.

Preparation of ZnO-Ag/CNCs Composites

ZnO-Ag/CNCs composite was synthesized with the initial suspension of CNCs in distilled water (100 mL, 2.0 wt %), then mixing it with zinc acetate dihydrate ($Zn(CH_3CO_2)_2.2H_2O$) in ethanol (50 mL, 10 wt %) with magnetic stirrer (Azizi *et al.*, 2013a). Afterward, 5.0 M sodium hydroxide solution (100 mL) was added drop-wise under continuous stirring at 80 °C until the pH of the solution was above 10 and a milky coloured suspension was obtained. Aqueous $AgNO_3$ solution (20 mL, 5.0 wt %) was then added with continuous stirring, and the reaction was continued for 2 h. The product was separated by centrifugation and carefully washed three times with distilled water. The final product was dried for 1 h at 100 °C for the complete transformation of the remaining zinc hydroxide to zinc oxide.

Characterization of CNCs, ZnO/CNCs, Ag/CNCs and ZnO-Ag/CNCs Composites

The FTIR spectra of CNCs, ZnO/CNCs, Ag/CNCs and ZnO-Ag/CNCs composites were obtained at ambient temperature using Perkin-Elmer FT-IR Spectrometer, Spectrum Two. 1 mg each of CNCs, ZnO/CNCs and ZnO-Ag/CNCs composites, and 1 mL of Ag/CNCs composites were placed in disks and scanned within a wave number range of 350 to 4000 cm^{-1}.

The UV-visible spectra of the materials were recorded over the range of 300 to 800 nm with UV-Visible (Shimadzu UV-2600 Spectrophotometer, Kyoto, Japan). 100 mg of CNCs, ZnO/CNCs and ZnO-Ag/CNCs composites were dissolved in 5 mL of ethanol while 2 mL of Ag/CNCs composites was diluted in 20 mL of ethanol, and aliquot placed in cuvettes and scanned in the UV-Vis spectrophotometer.

Antibacterial Activity of the Materials

CNCs, ZnO/CNCs, Ag/CNCs and ZnO-Ag/CNCs composites were evaluated for antibacterial activity against Gram-negative (*Escherichia coli*, *ATCC11229*, *Klebsiella pneumonia*, *BAA1705*, *Salmonella typhimurium*, *ATCC13311*, *Pseudomonas aeruginosa*, *ATCC15442*, *Enterococcus faecium*, *ATCC700221*, *Acinetobacter baumanii, MS01289518-1*) and Gram-positive (*Staphylococcus aureus, ATCC2600*, *S. aureus, 700699*, *S. aureus*, *71MRSA, S. epidermis, ATCC12228*, *Bacillus coagulans, UL02*, *Bacillus subtilis, UL01*, *Enterococcus faecalis, ATCC19433, E. faecalis*, *ATCC19437*) bacterial pathogens. The bacteria were grown in Muller-Hinton Agar medium for 24 h at 37 °C for 24 h. The plates were examined for presence of zones of inhibition which is indicated by clear area without microbial growth around the hole where drop of CNCs, ZnO/CNCs, Ag/CNCs and ZnO-Ag/CNCs suspension, ciprofloxacin and ethanol were placed in the plates. The diameters of inhibition zones were measured and the mean value for each organism was recorded.

Kinetics of Microbial Growth inhibition by the materials

Based on the results of antimicrobial activities' study, four strains (two gram positive and two gram negative) were studied for the rate of their growth inhibition by the materials. The pure culture of a standard strain of *Staphylococcus aureus (ATCC2600), Bacillus coagulans (UL02), Klebsiella pneumonia (BAA1705),* and *Salmonella typhimurium (ATCC13311)* were grown in nutrient broth at 37° C for 24 h to yield a cell count of 10^8cfu/mL. 1 mL

of each of the cultured bacteria strains were then added to 1.5L Eva® water bottles separately, to prepare the desired concentration of the bacteria solution. After 4 h, 1 mL of each of the suspension of CNCs, ZnO/CNCs, Ag/CNCs and ZnO-Ag/CNCs Composites (1 g of the composite materials dispersed in 10 mL of 70 % ethanol) was added to 200 mL of the prepared bacteria solution and 10 mL of the solution withdrawn into a cuvette in order to record rate of inhibition of microbial growth by optical density method using the absorbance at an interval of 1 h for 12 h in a UV-Vis spectrophotometer at a wavelength of 600 nm (Unuabonah *et al.*, 2017). Finally, 200 mL of the prepared bacteria solution in 0.75 L Eva water bottles without the suspension of the composites were taken as the controls. The measured absorbance from the UV-Vis spectrophotometer was related to the bacterial growth (cell count) with the expression: 1.0 Absorbance = 1 x 10^8 cfu/mL (Unuabonah *et al.*, 2017).

RESULTS AND DISCUSSION

Fourier Transforms Infrared (FTIR) Spectra of the Materials

FTIR measurements were carried out to identify the various functional groups in the biomolecules (CNCs) responsible for the reduction of $AgNO_3$, $Zn(CH_3CO_2)_2.2H_2O$ and acting as capping/stabilization agents for the sliver (Ag) and Zinc Oxide (ZnO) nanoparticles. The observed intense bands were compared with standard values to identify the functional groups. FTIR spectrum of CNCs are presented in Figure 1. The figure showed the following absorption bands and their corresponding functional groups: 3429.94 cm^{-1} (υ_s OH), 2923.81 cm^{-1} (υ_{as} CH_2 CH_3), 2854.05 cm^{-1} (υ_s CH_2 CH_3), 1745.5 cm^{-1} (υ_s C=O), 1634.65 cm^{-1} (υ_s C=C), 1200.51 cm^{-1} (υ_s S=O), 1055 cm^{-1} (υ_s C-O-C in pyranose ring), the spectra 721.76 cm^{-1} to 578.08 cm^{-1} represent the deformation, wagging and twisting modes of the hydroglucopyranose unit. The band at 1745.5 cm^{-1} was not prominent and was assigned for C=O stretching vibration due to the partial oxidation by sodium hypochlorite during the delignification, which introduced a few carboxylic acid groups on the surface of CNCs. The band at 1634.65 cm^{-1} is characteristic of CNCs. It corresponds to the C=C produced in the CNC by the dehydration effects of the conc. H_2SO_4 on the alcoholic OH of the biomass cellulose during the hydrolytic reaction. The band at 1460.99 cm^{-1} was assigned to the O-H band vibration present in the hydroxyl linkages of the CNCs. The bands at 1376.35 cm^{-1} represents the deformation vibration of C-H group of the glucose unit while 1309.4 cm^{-1} were assigned to the O-H in-plane band vibration. The band at 1200.51 cm^{-1} corresponds to C-O stretching vibration. The band at 1055.02 cm^{-1} in the spectrum corresponds to C-O-C stretching vibration of the secondary alcohols and ethers in the pyranose ring skeleton of the cellulose backbone (Cherian *et al.*, 2008; Lu and Hsieh, 2010). The 878.99 cm^{-1} is characteristic of the -glycosidic link between glucose units (Prakash *et al.*, 2013) which indicates the saccharide structure in CNC.

Ag/CNCs composite FTIR spectrum (Figure 2) was completely different from the neat CNC's spectrum (Figure 1). It shows absorption bands at 3435.82 cm^{-1}, 2066.38 cm^{-1}, 1636.21 cm^{-1}, 1085.29 cm^{-1}, 631.69 cm^{-1}, 399.88 cm^{-1}, 360.08 cm^{-1}. The FTIR spectrum, explains the interaction of Ag nanoparticles with CNCs with a very broadband at 3435.82 cm^{-1} due to the stretching vibration of O-H groups, while the band at 2066.38 cm^{-1} was associated with C-H group. An absorption band that appeared at 1636.21 cm^{-1} was attributable to the stretching vibration of C=C as found in the CNC spectrum due to H_2SO_4 dehydration, the two bands seen at 1085.29 cm^{-1} and 1039.0 cm^{-1} are due to the presence of C-N (aliphatic amine) stretching vibration, which come as a result of the reduction of $AgNO_3$ to Ag on CNCs. The FTIR results indicate the presence of -OH, C=C, and –CH groups, which indicated that the Ag/CNCs composites contains hydroxyl and other groups that can be used for bonding of Ag to the CNCs. The FTIR spectrum of Ag/CNCs composites (Figure 2) also exhibited a weak stretching vibration band at 1085.29 cm^{-1} which corresponds to the C-N stretching vibration of amine group which was absent in the neat CNC (Figure 1). The band recorded at 1085.29 cm^{-1} expressed in Ag/CNCs composite indicated that the NO_3^- in the $AgNO_3$ was converted into amino groups are partially incorporated in the CNC during the

encapsulation and stabilization of Ag nanoparticles by the CNC. Therefore, the CNCs must have acted as a reducing agent, which reduces Ag^{+} to Ag and the amino group as a stabilizing agent in the synthesis of Ag nanoparticles.

The FTIR spectrum of ZnO/CNCs composite are presented in Figure 3. The weak bands at 3744.2 cm^{-1}, 2348.4 cm^{-1}, 2312.66 cm^{-1}, 2218.3 cm^{-1} and a sharp band at 665.28 cm^{-1} were however observed in ZnO/CNCs composite but absent in CNCs. Comparing Figure 3 with Figure 1, a new band at 449.05 cm^{-1} fingerprint region was distinctly observed and attributed to Zn-O stretching vibration, confirming the nanocrystalline-ZnO interaction in the composites Azizi *et al.*, (2013b). In addition, comparison of the FTIR spectra of ZnO/CNCs and CNCs revealed that the band intensity of C=O stretching vibration (1745.5 cm^{-1}) disappear, which was ascribed to new bond formation from the strong interactions between oxygen atoms of the carboxyl functional group on the surface of the CNCs with ZnO nanoparticles.

The formation of ZnO-Ag nanoparticles on CNCs was confirmed by FTIR spectral analysis which is shown in Figure 4. The spectrum of ZnO-Ag/CNCs composites show absorption bands that were similar to that of CNCs, ZnO-CNCs and Ag/CNCs which indicate the formation of the composite. The silver modified CNC has no band at 454.04 cm^{-1} but ZnO modified samples have indicating that there is no chemical bonding between silver and ZnO. On the other hand, in addition to the ZnO band, the silver modified ZnO shows a weak band at 571.08 cm^{-1} followed by the band corresponding to oxygen deficiency. The successful formation of ZnO-Ag composites was proposed to follow the reaction path that involves the sequential addition of Zinc acetate dihydrate and $AgNO_3$ as important steps for the formation of Ag nanoparticles on ZnO surface (Tian *et al.*, 2010). As presented in the equations 1 – 3, the reaction stages involve interactions of Zn^{2+} cations to form bonds with the negatively charged hydroxyl (OH^{-}) functional groups, through electrostatic interactions. This first stage reaction in the composite formation produce effects that control the size by inhibiting the agglomeration of metallic particles formed in the synthesis process. Thus, the nanoparticles which are synthesized with this CNCs as capping agent are expected to be ideally small. This reaction involved dropwise addition of NaOH (equation 1) resulting in $Zn(OH)_2$-CNCs being slowly formed which when subjected to thermal conditioning form ZnO-CNCs (equation 2). With the addition of $AgNO_3$ (equation 3), Ag^{+} ions are reduced to Ag nanoparticles in the ZnO-CNCs alkaline suspension to produce the desired nanocomposite (Tian *et al.*, 2010). It may be inferred from the FTIR spectroscopic study that the functional properties of CNCs are affected because of their interaction with Ag^{+} and Zn^{2+} ions.

$$Zn^{2+} - CNCs + 2OH^{-} \rightarrow Zn(OH)_2 - CNCs \quad (1)$$

$$Zn(OH)_2 - CNCs \xrightarrow{\Delta} ZnO - CNCs + H_2O \quad (2)$$

$$2ZnO - CNCs + 2Ag^{+} + 2OH^{-} \rightarrow ZnO - Ag - CNCs + H_2O + \frac{1}{2}O_2 \quad (3)$$

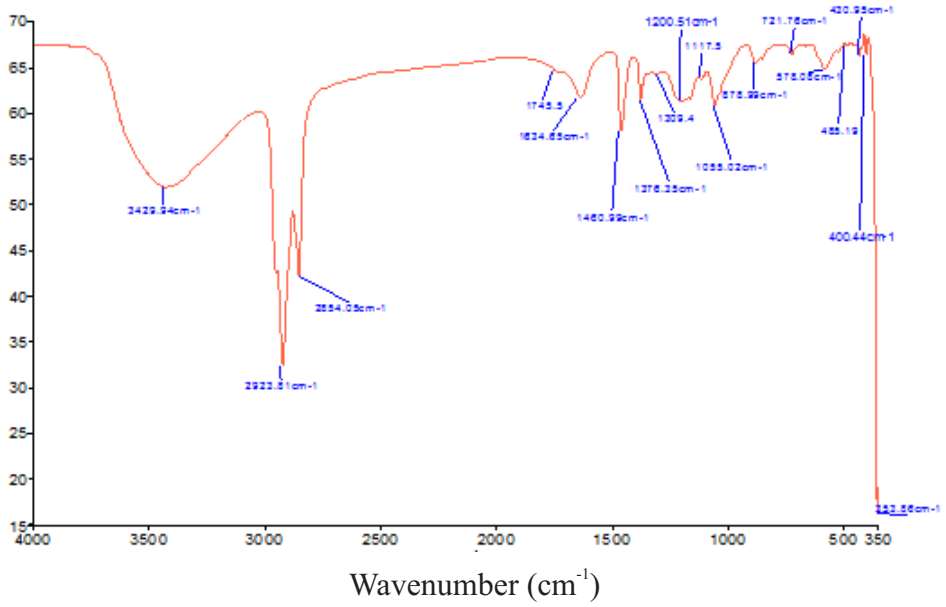

Figure 1: FTIR spectrum of CNCs.

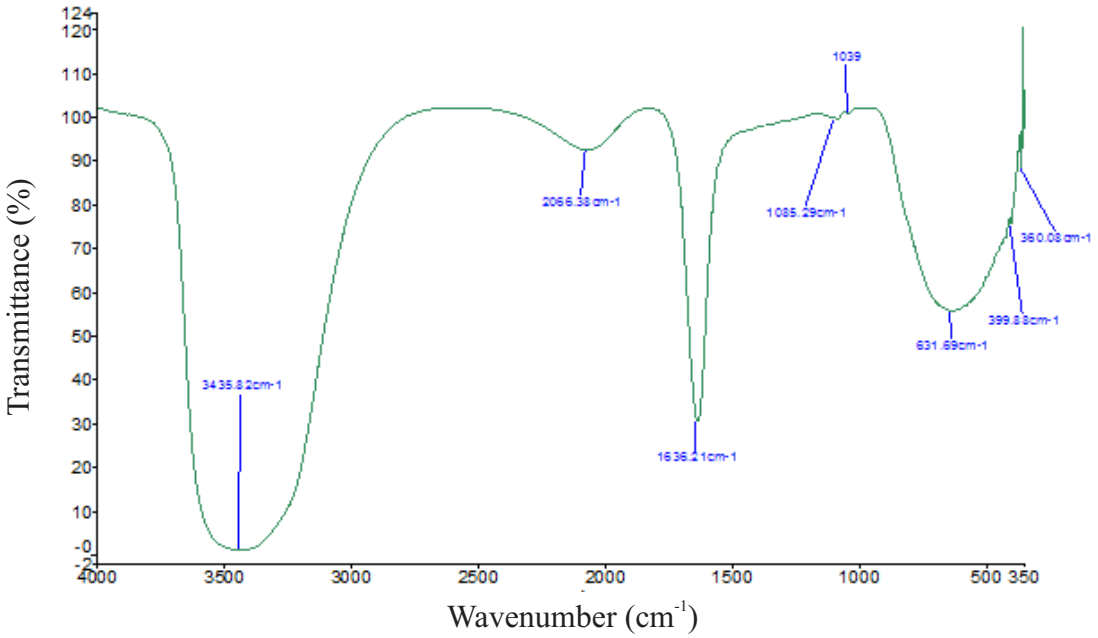

Figure 2: FTIR spectrum of Ag/CNCs composites.

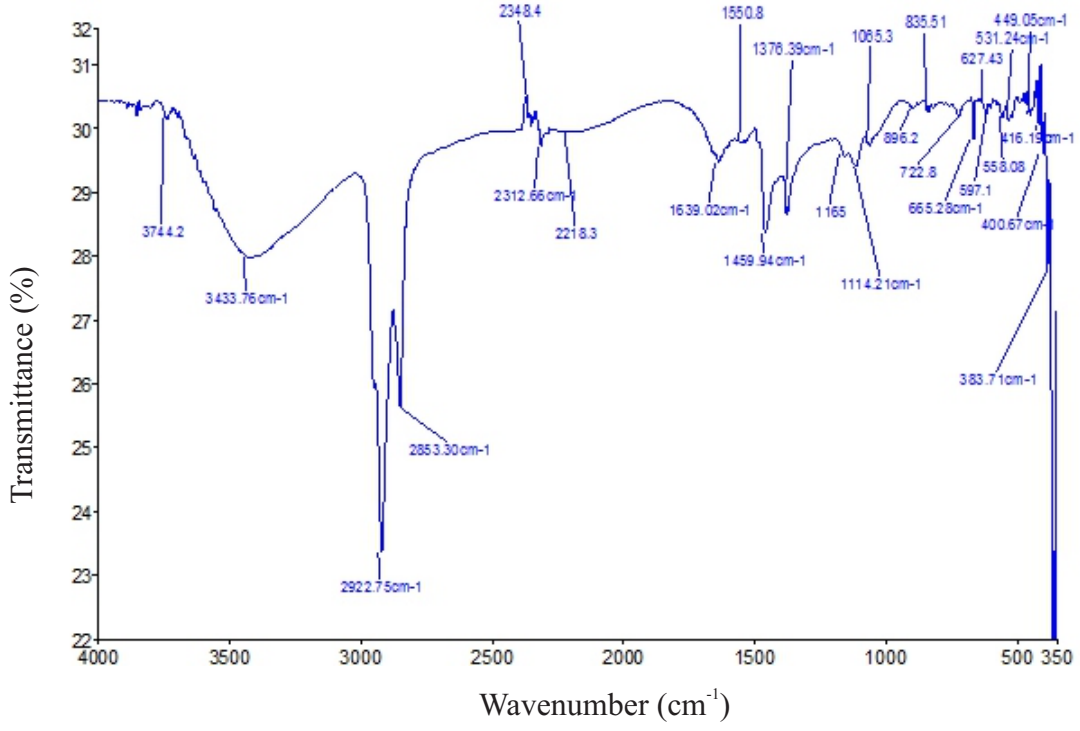

Figure 3: FTIR spectrum of ZnO/CNCs composites.

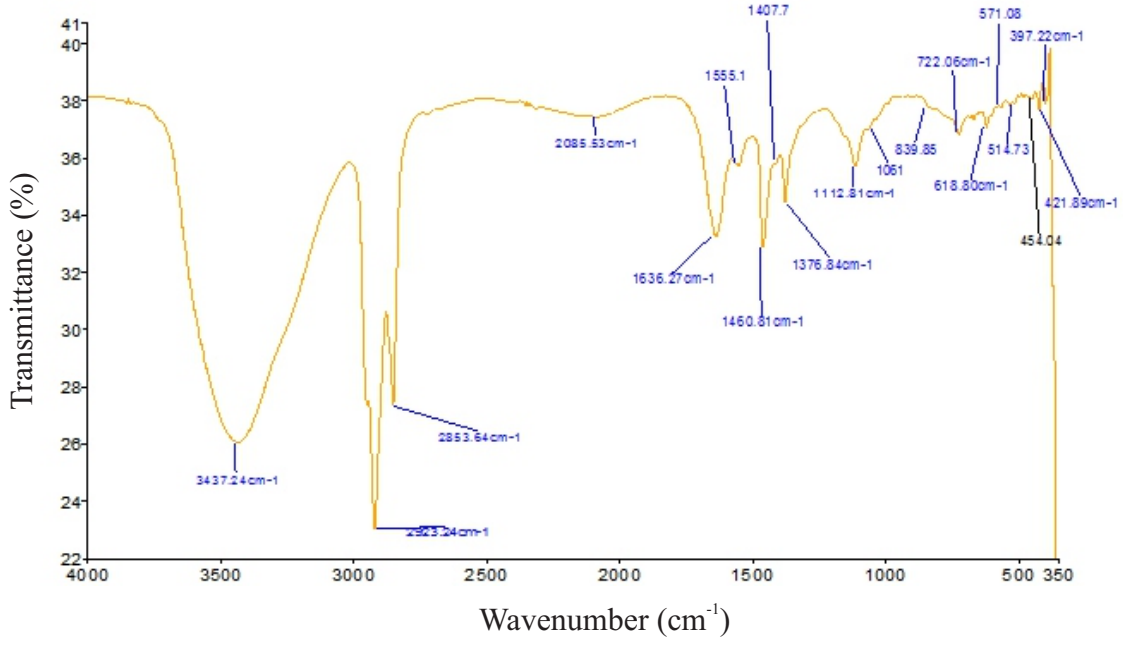

Figure 4: FTIR spectrum of ZnO-Ag/CNCs composites.

Ultraviolet Visible (UV-Vis) Absorbance Spectra of CNCs, ZnO/CNCs, Ag/CNCs and ZnO-Ag/CNCs Composites

The optical properties of CNCs, ZnO/CNCs, Ag/CNCs and ZnO-Ag/CNCs composites were characterized using a UV-Vis spectrophotometer. As shown in Figure 5, it was observed that there is no clear peak in the region of 300-800 nm in the spectrum of CNCs. CNC is not UV active because it does not contain extended conjugating bonds. The UV-Vis absorption spectra in Figure 5 of the Ag/CNCs composites showed a peak at 318.5 nm, which represents the localized plasmon resonance of the Ag nanoparticles deposited on CNCs. It was revealed that Ag/CNCs composites have optical activity as against CNCs that do not have as

depicted in the comparison of the UV-vis absorbance spectra of CNCs and Ag/CNCs composites (Figure 5).

The UV-Vis absorption spectrum of ZnO/CNCs composites showed a characteristic absorption peak at 316 nm, which could be ascribed to the basic band gap absorption of ZnO because of electron transitions from the valence to the conduction band (O 2p→Zn 3d) (Zak *et al.*, 2011). This confirms the formation of ZnO nanoparticles on the surface of CNCs. The UV-Vis absorbance spectrum of ZnO-Ag/CNCs composites recorded by UV-vis (Shimadzu UV-2600) spectrophotometer showed two absorption peaks at 316 and 348 nm corresponding to the band gap of the ZnO nanoparticles (Azizi *et al.*, 2014) and the surface plasmon resonance of the Ag NPs (Mulvaney, 1996), and these are clearly evident for ZnO-Ag/CNCs composites.

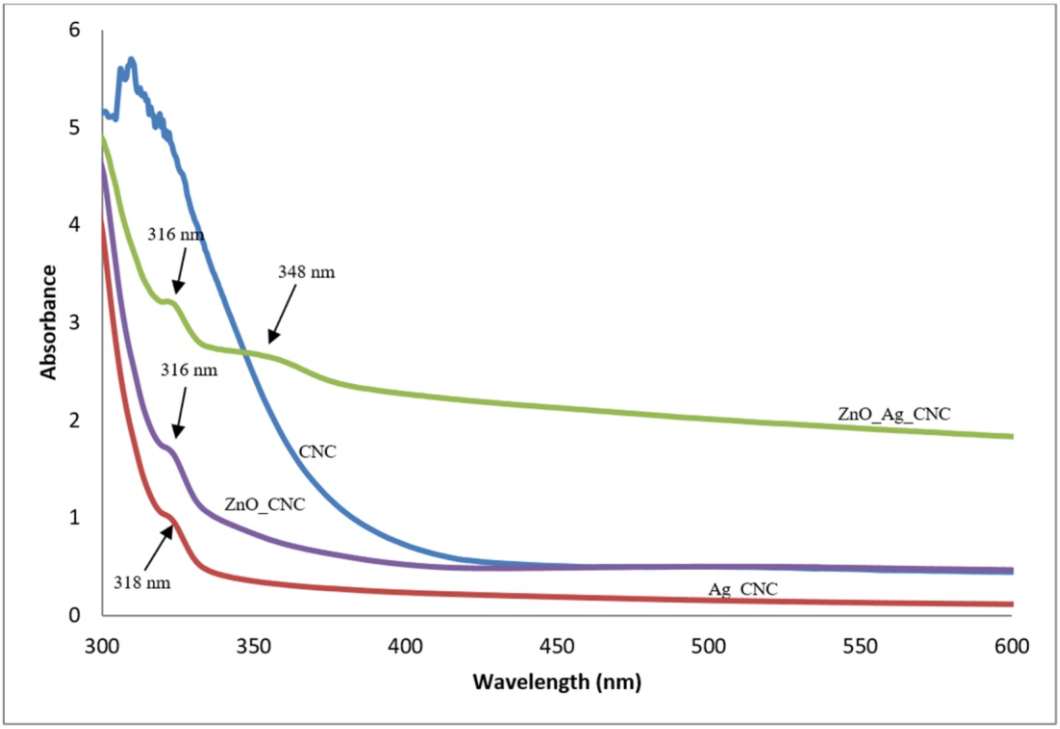

Figure 5: UV-vis absorbance spectra of CNCs and composites.

Antibacterial Activity of the Materials

The antibacterial activities of synthesized CNCs (B), ZnO/CNCs (C), Ag/CNCs (D) and ZnO-Ag/CNCs (A) composites were investigated against a range of pathogenic microorganisms using Muller-Hinton agar disk diffusion method and the results presented in Figure 6 – 9. Tables 1 and 2 showed the average diameters of the inhibition zone (mm) of the composites against Gram-negative and Gram-positive bacteria pathogens grown on Muller-Hinton Agar medium at 37 °C for 24 h. As shown in Tables 1 and 2, with the concentration (100 mg/mL) of CNCs (B), ZnO/CNCs (C), Ag/CNCs (D) and ZnO-Ag/CNCs (A) composites, the diameter of the inhibition zone is clearly observed, but it was observed in Figures 8 and 9 that Ag/CNCs (D) composites did not inhibit most of the bacteria used during the antibacterial test at high concentration (100 mg/mL). This is attributed to the low concentration of $AgNO_3$ used in the synthesis of Ag/CNCs (D) composites (5 mL of 5 mM),which correspond to very low Ag content (25 µmol). In Figures 6 and 7, it was observed that CNCs (B), ZnO/CNCs (C), Ag/CNCs (D) and ZnO-Ag/CNCs (A) composites did not inhibit the mentioned bacteria above at low concentrations (6.25, 12.5, 25.0, 50.0 µg/mL). This indicates the dose dependent activities of the material and expressed that effective concentration is higher. Ciprofloxacin and ethanol (E) were taken as control as shown in

Figures 6 and 7. Ciprofloxacin exhibited more antibacterial activity than ethanol (E). In this study, zone of inhibition was found to be highest (46 mm) against *S. epidermis* with CNC (B) at concentration of 100 mg/mL and lowest (9 mm) against *E. faecalis* with ZnO/CNC (C) composites at concentration of 100 mg/mL. These findings agreed with previous studies that investigated antibacterial activity of CNCs, ZnO/CNCs, Ag/CNCs and ZnO-Ag/CNCs composites (Ghosh *et al.*, 2012; Azizi *et al.*, 2013a).

The nanocrystal sizes and the resulting large surface area of the nanocomposite may have contributed to antibacterial enhancement. The antibacterial ability of CNCs, ZnO/CNCs, Ag/CNCs and ZnO-Ag/CNCs composites may also be related to their photocatalysis and metal release process (Wang *et al.*, 2004; Qin *et al.*, 2006). It has been documented that ZnO nanoparticles under light irradiation experience electron-hole pairs creation (Wang *et al.*, 2004; Qin *et al.*, 2006). The hole (h^+) reacted with OH^- on the surface of nanoparticles, generating hydroxyl radicals (HO_2.) These highly active free radicals harmed the bacterial cells resulting in decomposition and complete damage (Kikuchi *et al.*, 1997; Karunakaran *et al.*, 2010). It can be seen that the antibacterial ability of the CNCs, ZnO/CNCs and ZnO-Ag/CNCs nanocomposites were stronger against the Gram-positive bacteria (*S. aureus, 700699*, *Bacillus coagulans, UL02*) compared to the Gram-negative bacteria (*Escherichia coli*, *ATCC11229*, *Salmonella typhimurium*, *ATCC13311*, *Enterococcus faecium*, *ATCC700221*, *Acinetobacter baumanii, MS01289518-1*). Kikuchi *et al.*, (1997) also documented stronger antibacterial power of TiO_2 photocatalyst against Gram-positive bacteria. The lower effect on Gram-negative bacteria may be attributed to the fact that their cell walls contain an external lipopolysaccharide (LPS) membrane that shields the peptidoglycan layer. Furthermore, Ag, ZnO and ZnO-Ag nanoparticles without CNCs displayed a less powerful influence toward Gram-positive and negative bacteria in comparison to ZnO/CNCs, Ag/CNCs and ZnO-Ag/CNCs composites which suggests that CNCs may have assisted in the passage of the nanocomposites in the membrane barrier to create higher influence. Our study therefore suggests that the antibacterial activity of CNCs, ZnO/CNCs, Ag/CNCs and ZnO-Ag/CNCs composites could be the result of a high contact of the well dispersed and stabilized nanoparticles with higher tendency of membrane barrier passage into the bacteria, through a tight joining of CNCs to the bacterial envelope.

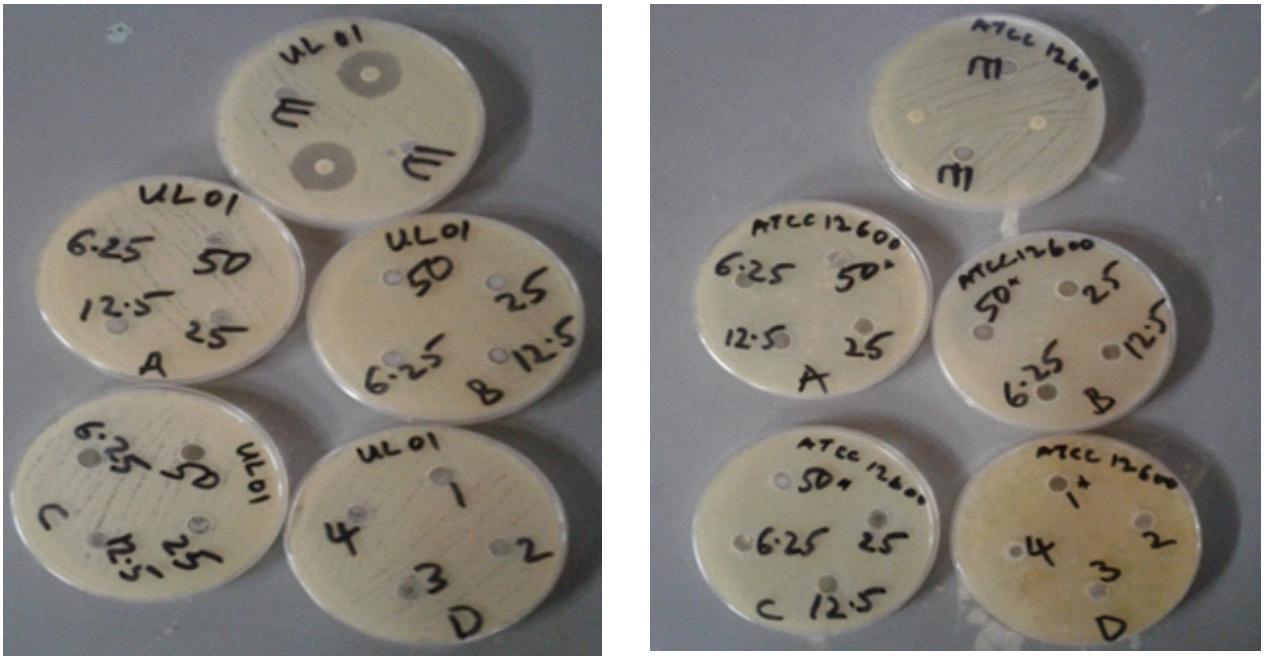

Bacillus subtilis *Staphylococcus aureus*

Figure 6: Inhibition zone of CNCs (B), ZnO/CNCs (C), Ag/CNCs (D) andZnO-Ag/CNCs (A) composites at low concentrations (6.25, 12.5, 25.0, 50.0 µg/mL) against Gram-positive bacteria.

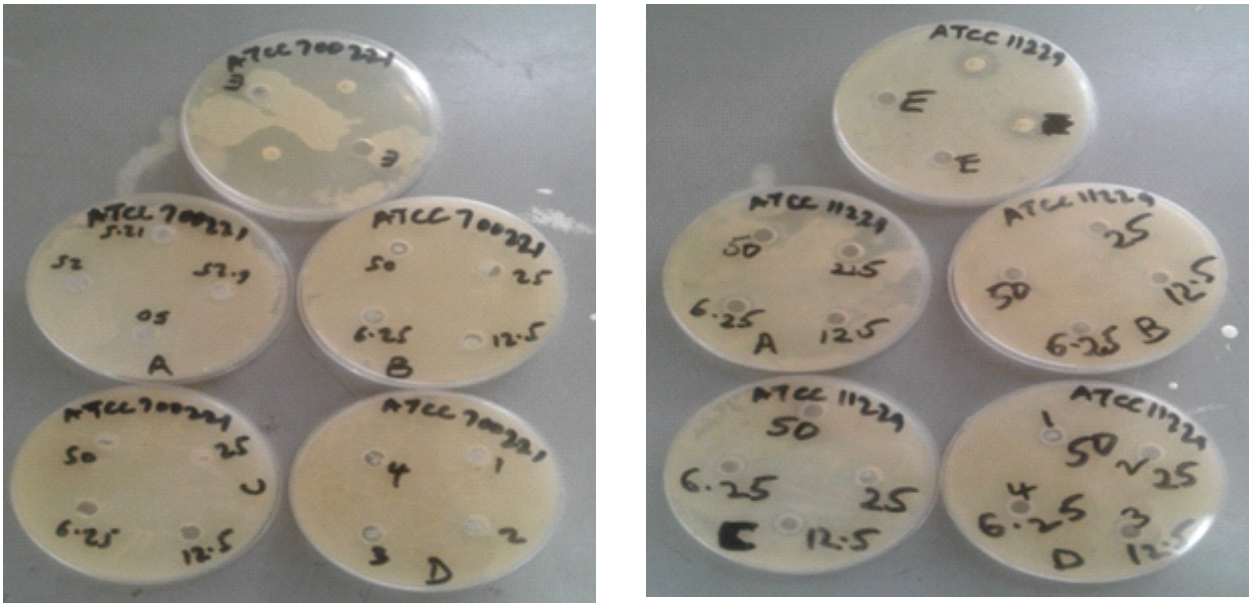

Enterococcus faecium *Escherichia coli*

Figure 7: Inhibition zone of CNCs (B), ZnO/CNCs (C), Ag/CNCs (D) andZnO-Ag/CNCs (A) composites at low concentrations (6.25, 12.5, 25.0, 50.0 µg/mL) against Gram-negative bacteria.

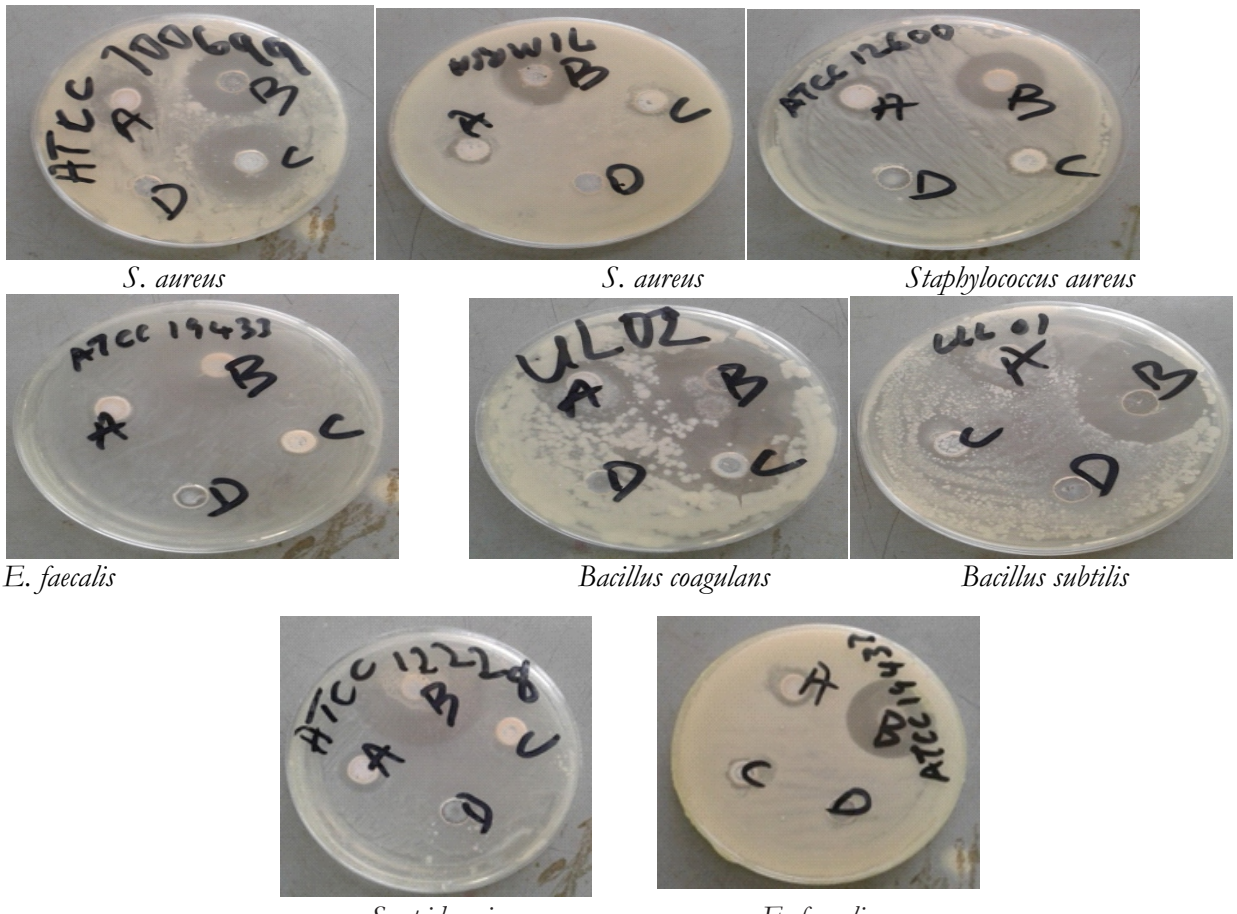

S. aureus *S. aureus* *Staphylococcus aureus*

E. faecalis *Bacillus coagulans* *Bacillus subtilis*

S. epidermis *E. faecalis*

Figure 8: Inhibition zone of CNCs (B), ZnO/CNCs (C), Ag/CNCs (D) and ZnO-Ag/CNCs (A) composites at high concentration (100 mg/mL) against Gram-positive bacteria.

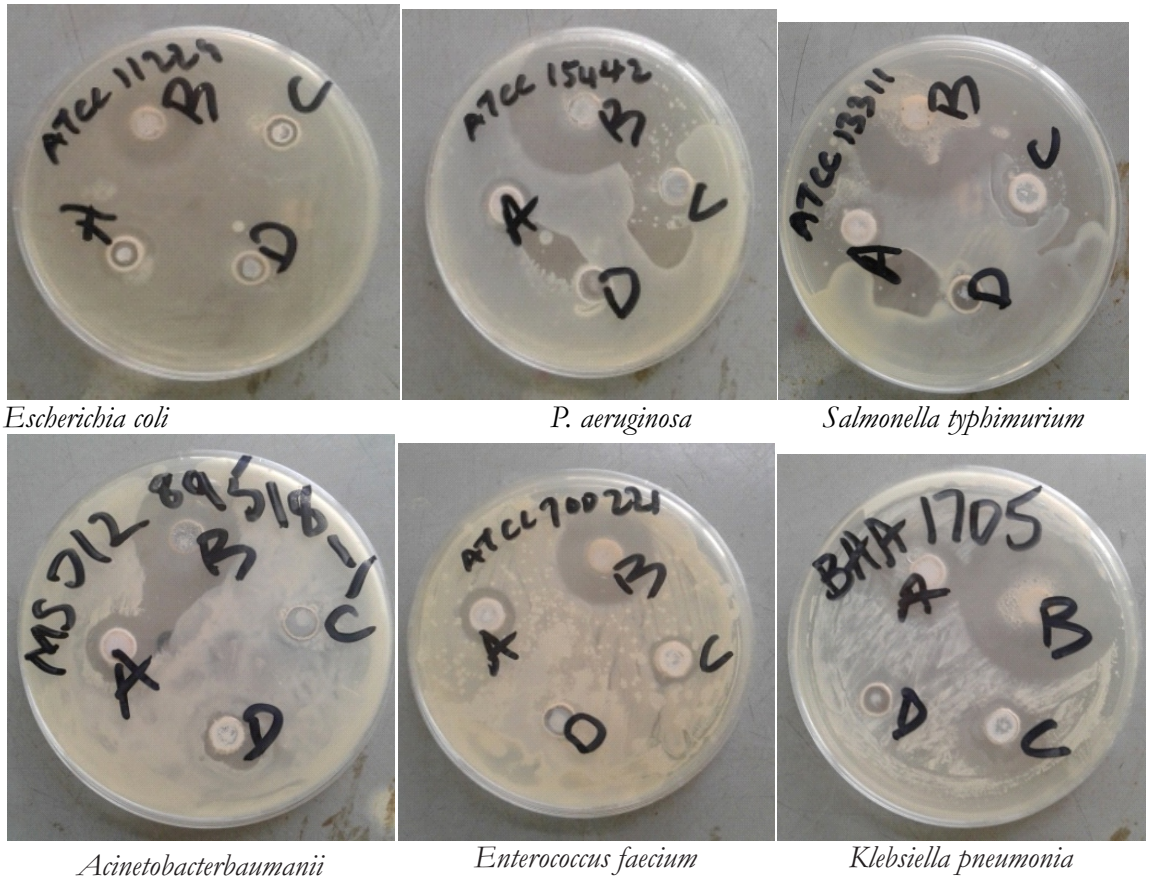

Escherichia coli *P. aeruginosa* *Salmonella typhimurium*

Acinetobacterbaumanii *Enterococcus faecium* *Klebsiella pneumonia*

Figure 9: Inhibition zone of CNCs (B), ZnO/CNCs (C), Ag/CNCs (D) and ZnO-Ag/CNCs (A) composites at high concentration (100 mg/mL) against Gram-negative bacteria.

Table 1: Inhibition zone of CNCs (B), ZnO/CNCs (C), Ag/CNCs (D) and ZnO-Ag/CNCs (A) composites at high concentration (100 mg/mL) against Gram-positive bacteria.

		Diameter of zone of Inhibition (mm)			
Gram-Positive Bacteria	**Strain or Code type**	**CNCs (B)**	**ZnO/CNCs (C)**	**Ag/CNCs (D)**	**ZnO-Ag/CNCs (A)**
Staphylococcus aureus	*ATCC 2600*	22.0	11.0	Null	15.0
S. aureus	*700699*	26.5	26.0	Null	16.5
S. aureus	*71MRSA*	21.5	12.0	Null	11.5
S. epidermis	*ATCC12228*	46.0	Null	Null	14.0
Bacillus coagulans	*UL02*	30.0	24.0	Null	23.0
Bacillus subtilis	*UL01*	31.0	14.0	Null	Null
E. faecalis	*ATCC 19433*	Null	9.0	Null	11.0
E. faecalis	*ATCC 19437*	26.0	10.0	Null	13.0

Table 2: Inhibition zone of CNCs (B), ZnO/CNCs (C), Ag/CNCs (D) and ZnO-Ag/CNCs (A) composites at high concentration (100 mg/mL) against Gram-negative bacteria.

		Diameter of zone of Inhibition (mm)			
Gram-Negative Bacteria	**Strain or Code type**	**CNCs (B)**	**ZnO/CNCs (C)**	**Ag/CNCs (D)**	**ZnO-Ag/CNCs (A)**
Escherichia coli	*ATCC 11229*	20.0	Null	Null	13.0
Klebsiella pneumonia	*BAA 1705*	37.5	15.0	Null	22.5
Salmonella typhimurium	*ATCC 13311*	Null	13.0	Null	12.5
P. aeruginosa	*ATCC15442*	40.0	13.0	Null	13.0
Enterococcus faecium	*ATCC 700221*	25.0	11.5	Null	14.0
Acinetobacterbaumanii	*MS01289518-1*	25.0	Null	13.5	14.5

Kinetics of inhibitory actions of the composite materials on selected bacterial growth rate

The kinetics of actions of synthesized composite materials on the growth of *S. aureus (ATCC2600), Bacillus coagulans (UL02), Klebsiella pneumonia (BAA1705)* and *Salmonella typhimurium* (ATCC 13311) were investigated using optical density method and the results presented in Table 3 based on rate constants k_1 and k_2 for first and second order reaction rate laws respectively and the degree of fitness (R^2) into the rate laws. Generally, the observed trend of the growth first order rate of the bacteria in the untreated water was *S. aureus* (0.546 h^{-1}) >*Klebsiella pneumonia* (0.2639 h^{-1}) >*Bacillus coagulans* (0.125 h^{-1}) >*Salmonella typhimurium* (0.0410 h^{-1}).

For *S. aureus (ATCC2600)*, the inhibition rate in water alone and water treated with CNC fits into the first order rate law but the inhibition rate by the Ag/CNCs, ZnO/CNCs and ZnO-Ag/CNCs treated water was best explained by the second order rate law. It therefore implies that the composite materials contribute to the rate law in the water samples treated with the materials. A comparison of the rate constants (k_1 and k_2) within the untreated water and the treated water clearly showed a significant reduction in the rate constant which is the clear evidence of the inhibition by the added composite. The first order rate constant (k_1) of untreated water was 0.546 h^{-1} but that of the composite treated ranged between 0.0195 – 0.0743 h^{-1}. This growth rate of *S. aureus* in the untreated water was between 28 times (0.0195 h^{-1}) and 10 times (0.0743 h^{-1}) faster than in the treated water which implies that the composite materials can inhibit the growth of the bacteria for over 10 h when applied as disinfectant. The undoped CNCs inhibit better than even the doped. The second other rate constant also support this observed inhibitory activity of the composite material. In the untreated water, the second order rate constant (k_2) was $1x10^{-5}$ $(cfu)^{-1}mLh^{-1}$ which is a hundred magnitude higher than the $1x10^{-7}$ $(cfu)^{-1}mLh^{-1}$ rate constant obtained for water treated with CNCs. The rate constant of the water treated with Ag and ZnO singly doped materials was even much lower in magnitude ($6x10^{-8}$ $(cfu)^{-1}mLh^{-1}$) to the CNCs treated and the composite of ZnO-Ag/CNCs far much lower. It can be clearly inferred that the treatment of the *S. aureus* contaminated water with the composite materials created an inhibition in the growth of the *S. aureus* with better inhibition by the ZnO-Ag/CNCs composite. This affirms the disinfectant potentials of ZnO-Ag bimetallic composite (Karunakaran *et al*., 2010) and the synergistic impact of ZnO-Ag/CNCs composite.

The result of the inhibition actions of the composite materials on *Bacillus coagulans (UL02)*as presented in Table 3 revealed that the ZnO doped treated water fits more of first order rate law while the untreated and CNCs treated fits the second order rate law. The Ag treated fits equally into both. The first order rate constant of the *Bacillus coagulans* contaminated untreated water was 0.125 h^{-1} which 28 times faster than the 0.0044h^{-1} obtained for the CNCs treated water and the 0.0079 – 0.017 h^{-1} obtained for the Ag and ZnO composite treated ones. There is a likelihood of

these materials inhibiting the growth of *Bacillus coagulans* for up till between 15 to 28 h if applied as disinfectant. The inhibition rate of CNCs alone on *Bacillus coagulans* is higher than the Ag and ZnO doped ones which is similar to the result obtained for *S. aureus*. In the second order rate law of the materials' inhibition of *Bacillus coagulans* growth, it can be deduced that the growth rates of the treated water were lower by thousands and tens of thousand times than in the untreated water. Comparatively, the materials seem to slightly inhibit the growth rate of *Bacillus coagulans* more than the growth rate of *S. aureus*.

Klebsiella pneumonia (BAA1705) first order growth rate constant in untreated water was 0.2639 h^{-1} at $R^2 = 0.9849$. This rate is just 4 time slower that the 0.0609 h^{-1} at $R^2 = 0.8243$ obtained for the CNCs treated water. The growth rate in the Ag treated was 7 times slower that the untreated water (0.0374 h^{-1} at $R^2 = 0.8454$) while the ZnO and the Ag-ZnO doped treated exhibit 10 times slower growth rate. This is a departure from the trend observed in *B. coagulans* and *S. aureus*. The undoped CNCs were not able to significantly inhibit the growth of *K. pneumonia* but the doping assisted in increasing the inhibition rate till 10 times. It may be hypothesized that the application of these materials to inhibit the growth of *K. pneumonia* may only work for maximum of 7 h as against the over 10 h obtained for *B. coagulans* and *S. aureus*. The second order rate law results of *K. pneumonia* also showed thousands and tens of thousand times slower cfu growth rate in the treated than in the untreated water.

Finally, the growth rate of *Salmonella typhimurium (ATCC 13311)* as presented in Table 3 should a higher first order growth rate in untreated water (0.0410 h^{-1} at $R^2 = 0.8006$) than in the CNCs treated water (0.0040 h^{-1} at $R^2 = 0.8127$). The action of CNCs on the growth of *Salmonella*

Table 3: Kinetics of inhibitory actions of CNCs, ZnO/CNCs, Ag/CNCs, and ZnO-Ag/CNCs composites on *the bacteria*

Order of Reaction		***S. aureus (ATCC2600) +***				
		H_2O (E)	H_2O + CNCs (B)	H_2O + Ag/CNCs (D)	H_2O + ZnO/CNCs (C)	H_2O + ZnO-Ag/CNCs (A)
First	k_1/h^{-1}	0.546	0.0195	0.0511	0.0743	0.0230
Order	R^2	0.8960	0.8826	0.6958	0.7811	0.7370
Second	$k_2/(cfu)^{-1}mLh^{-1}$	$1x10^{-5}$	$1x10^{-7}$	$6x10^{-8}$	$6x10^{-8}$	$4x10^{-9}$
Order	R^2	0.8016	0.8122	0.7620	0.8032	0.8286
Order of Reaction		***Bacillus coagulans (UL02) +***				
		H_2O (E)	H_2O + CNCs (B)	H_2O + Ag/CNCs (D)	H_2O + ZnO/CNCs (C)	H_2O + ZnO-Ag/CNCs (A)
First	k_1/h^{-1}	0.125	0.0044	0.0079	0.0144	0.0170
Order	R^2	0.8103	0.8128	0.8120	0.9939	0.9701
Second	$k_2/(cfu)^{-1}mLh^{-1}$	$5x10^{-5}$	$4x10^{-8}$	$7x10^{-9}$	$3x10^{-9}$	$3x10^{-9}$
Order	R^2	0.8518	0.8258	0.8171	0.9727	0.9400
Order of Reaction		***Klebsiella pneumonia (BAA1705) +***				
		H_2O (E)	H_2O + CNCs (B)	H_2O + Ag/CNCs (D)	H_2O +ZnO/CNCs (C)	H_2O +ZnO-Ag /CNCs (A)
First	k_1/h^{-1}	0.2639	0.0609	0.0374	0.0254	0.0250
Order	R^2	0.9849	0.8243	0.8454	0.8479	0.9264
Second	$k_2/(cfu)^{-1}mLh^{-1}$	$2x10^{-5}$	$3x10^{-8}$	$4x10^{-8}$	$7x10^{-9}$	$4x10^{-9}$
Order	R^2	0.9913	0.8287	0.9431	0.9000	0.9483
Order of Reaction		***Salmonella typhimurium (ATCC13311)+***				
		H_2O (E)	H_2O + CNCs (B)	H_2O + Ag/CNCs (D)	H_2O + ZnO/CNCs (C)	H_2O + ZnO-Ag/CNCs (A)
First	k_1/h^{-1}	0.0410	0.0040	0.0261	0.0023	0.0047
Order	R^2	0.8006	0.8127	0.8583	0.8177	0.9300
Second	$k_2/(cfu)^{-1}mLh^{-1}$	$3x10^{-5}$	$1x10^{-8}$	$4x10^{-7}$	$4x10^{-10}$	$1x10^{-10}$
Order	R^2	0.9686	0.9308	0.9769	0.8242	0.9727

typhimurium is 10 times inhibition as against the 28 times witnessed in *B. coagulans* and *S. aureus* and 4 times inhibition witnessed on *K. pneumonia*. This presupposes that CNCs has better inhibition action rate of gram positive bacteria than on gram negative. The inhibition rate of Ag-CNCs treatment was poor on *S. typhimurium* (k_1 = 0.0261 h^{-1}) being less that twice reduction on the untreated. ZnO and Ag-ZnO doped CNCs had better first order inhibition rate on the growth of *S. typhimurium* with 0.0023 and 0.0047 h^{-1} respectively. This translates to 17 times and 8 times inhibition respectively compared to the untreated water. It may therefore be implied that the materials can inhibit the growth of *S. typhimurium* for 8 to 17 h. There are indications that the addition of ZnO improved the bacteria inhibition better than the Ag.

CONCLUSION

The CNCs acted as capping agent for the ZnO/CNCs, Ag/CNCs and ZnO-Ag/CNCs composites production. The composites characterization indicated changes in the functional grouption of the composites. The CNCs and the composite materials were found to exhibit antibacterial properties at 100 mg/mL with clear zone of inhibition from 9-46 mm. The kinetic studies showed the growth rate of the bacteria to be first order in the untreated water and the rate constants were found to follow the trend *S. aureus* (0.546 h^{-1}) >*Klebsiella pneumonia* (0.2639 h^{-1}) >*Bacillus coagulans* (0.125 h^{-1}) >*Salmonella typhimurium* (0.0410 h^{-1}). A significant reduction in the growth rates of the CNCs and the composites' treated water was observed with the rate constants shown to be 4 to 28 times lower than their corresponding untreated water. This implies that the bacteria growth may be impeded for 4 to 28 h depending on the bacteria and the material applied. The materials studied showed better growth inhibition rate for gram positive bacteria than gram negative. These materials and their composites (CNCs, ZnO/CNCs, Ag/CNCs and ZnO-Ag/CNCs) may be applied in personal care products, antiseptic solutions or, more concentrated, in wound-healing gels and other external uses as alternatives to chlorophenols that is not eco-friendly.

ACKNOWLEDGEMENTS

The authors acknowledged the assistance of Mr. Ogah and Mr. Achem of the University of Lagos Microbiology and Chemistry laboratories, respectively.

AUTHORS' CONTRIBUTIONS

FOA: conceptualization; supervision; data curation; formal analysis; validation; visualization; manuscript preparation. EEA: investigation; methodology; resources; formal analysis; visualization; manuscript preparation. GOO: conceptualization; supervision; data curation; formal analysis; manuscript preparation.

REFERENCES

Alexandre, M.; Dubois, P. (2000). Polymer-Layered Silicate Nanocomposites: Preparation, Properties and Uses of a Class of Materials. *Materials Science and Engineering: R: Reports*, 28, 1-63.

Armentano, I.; Del-Gaudio, C.; Bianco, A.; Dottori, M.; Nanni, F.; Fortunati, E. (2009). Processing and Properties of Poly(e-Caprolactone)/Carbon Nanofibre Composite Materials and Films Obtained by Electrospinning and Solvent Casting. *Journal of Material Science*, 44, 4789-4795.

Azizi, S.; Ahmad, M. B.; Abdolmohannadi, S. (2013b). Preparation, Characterization, and Antimicrobial Activities of ZnO Nanoparticles/Cellulose Nanocystal nanohybrid. *BioResources*, 8, 1841-1851.

Azizi, S.; Ahmad, M. B.; Hussein, M. Z.; Ibrahim, N. A. (2013a). Synthesis, Antibacterial and Thermal Studies of Cellulose Nanocrystal Stabilized ZnO-Ag Heterostructure Nanoparticles. *Molecules*, 18, 6269-6280.

Azizi, S.; Ahmad, M. B.; Namvar, F.; Mohamad, R. (2014). Green Biosynthesis and Characterization of Zinc Oxide Nanoparticles using Brown Marine Macroalga *Sargassum muticum* Aqueous Extract. *Material Lett*ers, 116, 275-277.

Azubuike, C. P.; Okhamafe, A. O.; Falodun, A. (2011). Some Pharmacopoeial and Diluent-Binder Properties of Cellulose Derived from Maize Cob in Selected Tablet Formulations. *J. Chem. Pharm. Res.,* 3, 481-488.

Bianco, A.; Di Federico, E.; Moscatelli, I.; Camaioni, A.; Armentano, I.; Campagnolo, L.(2009). Electrospum Poly (3-Caprolactone)/Ca-Deficient Hydroxyapatite Nanohybrids: Microstructure, Mechanical Properties and Cell Response by *Murine embryonic* Stem Cells. *Material Science and Engineering*, C29, 2063-2071.

Chae, H.; Young Bum, L.; Jim Woo, B.; Jae Young, J.; Byeong U.N.; Tae Won, H. (2005). Preparation and Mechanical Properties of Propylene/Clay Nanocomposites for Automotive Parts Application. *Journal of Applied Polymer Science*, 98(1), 427-433.

Chaudhary, S., Jain, V.P., Sharma, D.., and Jaiswar, G. (2023). Implementation of agriculture waste for the synthesis of metal oxide nanoparticles: its management, future opportunities and challenges. J Mater Cycles Waste Manag 25, 3144–3160.

doi: 10.1007/s10163-023-01770-0

Chen, R.Q.; Zou, C. W.; Bian, J. M.; Sandhu, A.; Gao, W. (2011). Microstructure and Optical Properties of Ag-doped ZnO Nanostructures Prepared by a Wet Oxidation Doping Process. *Nanotechnology,* 22, 105706-105713.

Cherian, B. M.; Pothan, L. A.; Nguyen-Chung, T.; Menning, G.; Kottaisamy, M.; Thomas, S. (2008). A Novel method for the Synthesis of Cellulose Nanofibril Whiskers from Banana Fibers and Characterization. *J. Agric. Food Chem.,* 56, 5617-5627.

Debeaufort, F.; Quezaba-Gallo, J. A.; Voilley, A. (1998). Edible Films and Coatings: Tomorrow's Packaging's. *Critical Reviews in Food Science and Nutrition*, 38, 299-313.

Drogat, N.; Granet, R.; Sol, V.; Memmi, A.; Saad, N.; Koerkamp, C.; Bressollier, P.; Krausz, P. (2011). Antimicrobial Silver Nanoparticles Generated on Cellulose Nanocrystals. *Journal of Nanoparticles Resources,* 13, 1557-1562.

Ghosh, S.; Patil, S.; Ahire, M.; Kitture, R.; Kale, S.; Pardesi, K. (2012).Synthesis of Silver Nanoparticles Using *Dioscorea bulbifera* Tuber Extract and Evaluation of its Synergistic Potential in Combination with Antimicrobial Agents. *International Journal of Nanomedicine*, 7, 483-496.

Gorrasi, G.; Vittoria, V.; Murariu, M.; Ferreira, A. D. S.; Alexandre, M.; Dubois P. (2008). Effect of Filler Content and Size on Transport Properties of Water Vapor in PLA/Calcium Sulfate Composites. *Composite Science Technology*, 9, 627-632.

Habibi, Y.; Lucia, L. A.; Rojas, O. J. (2010). Cellulose Nanocrystals: Chemistry, Self Assembly, and Applications. *Chemical Reviews* ,110, 3479-3500.

Hong, J. F.; Mato, K.; Roland, S.; Kornelius, N.; Eckhard, P.; Dietrich, H.; Margit, Z.; Ulrich, G. (2006). Monocrystalline Spinel Nanotube Fabrication Based on the Kirkendall Effect. *Nature Material,* 5, 627-631.

Karunakaran, V.; Rajeswari, P.; Sankar, G. (2010). Antibacterial and photocatalytic activities of sonochemically prepared ZnO and Ag-ZnO. *J. Alloys Compd.,* 508, 587-591.

Kikuchi, Y.; Sunada, K.; Iyoda, T.; Hashimoto, K.; Fujishima, A. (1997). Photocatalytic bactericidal effect of TiO_2 Thin Films: Dynamic View of the Active Oxygen Species Responsible for the effect. *J. Photochem. Photobiol. A Chem.,* 106, 51-56.

Kim, D.; Jeon, K.; Lee, Y.; Seo, K.; Han, H.; Khan, Sh. B. (2012). Preparation and Characterization of UV-cured Polyurethane Acrylate/ZnO Nanocomposite Films Based on Surface Modified ZnO. *Progress in Organic Coatings*, 74, 435-442.

Koh, H. C.; Park, J. S.; Jeong, M. A.; Hwang, H. Y.; Hong, Y. T. (2008). Preparation and Gas Permeation Properties of Biodegradable Polymer/Layered Silicate Nanocomposite Membranes. *Desalination*, 233, 201-209.

Kvien, I.; Tanem, B. S.; Oksman, K. (2005).Characterization of Cellulose Whiskers and Their Nanocomposites by Atomic Force and Electron Microscopy. *Biomacromolecules*, 56, 3160-3165.

Kylma, J.; Tuominen, J.; Helminen, A.; Seppala, J. (2001).Chain Extending of Lactic Acid Oligomers. Effect of 2,2-Bis (2-Oxazoline) on 1,6-Hexamethylene Diisocyanate Linking Reaction. *Polymer* , 42(8), 3333-3343.

Lateef, A., Azeez, M.A., Asafa, T.B., Yekeen, T.A., Akinboro, A., Oladipo, I.C., Azeez, L., Ajibade, S.E., Ojo, S.A., Gueguim-Kana, E.B., Beukes, L.S. (2016). Biogenic synthesis of silver nanoparticles using a pod extract of *Cola nitida*: antibacterial, antioxidant activities and application as a paint additive, J. Taibah Univ. Sci. 10 (4), 551–562.

Lu, P.; Hsieh, Y. (2010). Preparation and Properties of Cellulose Nanocrystals: Rods, Spheres and Network. *Carbohydrate Polym*er, 82, 329-336.

Mali, P. and Sherje, A.P. (2022). Cellulose nanocrystals: Fundamentals and biomedical applications. Carbohydrate Polymers 275, 118668. doi: 10.1016/j.carbpol.2021.118668

Marsh, K.; Bugusu, B. (2007).Food Packaging: Roles, Materials and Environmental Issues. *Journal of Food Science*, 72, 39-55.

Mulvaney, P. (1996). Surface Plasmon Spectroscopy of Nanosized Metal Particles. *Langmuir*, 12,788-800.

Olabemiwo, O.M., Lateef, A., Agunbiade, F.O., Akanji, S.B. and Bakare, H. O. 2020. Theeffects on oxidative aging, physical and flow properties of Agbabu natural bitumen modified with silver nanoparticles. Heliyon 6(6), e04164. doi: 10.1016/j.heliyon.2020.e04164.

Padalkar, S.; Capadona, J. R.; Rowan, S. J.; Weder, C.; Won, Y. H.; Stanciu, L. A.; Moon, R. J. (2010). Natural bio-Polymers: Novel Templates for the Synthesis of Naonstructures. *Langmuir*, 26, 8497-8502.

Peponi, L.; Terejak, A.; Torre, L.; Mondragon, I.; Kenny, J. M. (2009).Nanostructured Physical Gel of SBS Block Copolymer and Ag/DT/SBS Nanocomposites. *Journal of Material Science*, 44, 1287-1293.

Prakash, P.; Gnanaprakasam, P.; Emmanuel, R.; Arokiyaraj, S.; Saravanan, M. (2013). Green Synthesis of Silver Nanoparticles from Leaf Extract of *Mimusopselengi*, Linn. for Enhanced Antibacterial Activity against Multi Drug Resistant Clinical Isolates. *Colloids and Surfaces B: Biointerfaces,* 108, 255-259.

Qin, Y. M.; Zhu, C. J.; Chen, J.; Chen, Y. Z.; Zhang, C. (2006). The Absorption and Release of Silver and Zinc Ions by Chitosan Fiber. *Journal of Applied Science.,* 101, 766-771.

Raman, N.; Sudharsan, S.; Pothiraj, K. (2011).Synthesis and Structural Reactivity of Inorganic-Organic Hybrid Nanocomposites-A review. *Journal of Saudi Chemical Society*, 16, 339-352.

Rasato, D. (2009). The Emerging World of Bio-Plastics: An Industry ``Father" looks Forward. *http:www.omnexus.com/resources/print.aspx/id=22050*.

Ray, S. S.; Bousmina, M. (2005). Biodegradable Polymers and their Layered Silicate Nanocomposites: In Greening the 21st Century Materials World. *Progress in Materials Science*, 50(8), 962-1079.

Sarkar, J., Mridha, D., Sarkar, J., Orasugh, J.T., Gangopadhyay, B., Chattopadhyay, D., Roychowdhury, T., Acharya, K. (2021). Synthesis of nanosilica from agricultural wastes and its multifaceted applications: A review. *Biocatalysis and Agricultural Biotechnology*, 37, 102175, doi: 10.1016/j.bcab.2021.102175.

Shinsuke, I.; Manami, T.; Minoru, M.; Hiroyuki, S.; Hiroyuki, Y. (2009). Synthesis of Silver Nanoparticles Templated by TEMPO-Mediated Oxidized Bacterial Celloluse Nanofibers. *Biomacromolecules*, 10, 2714-2717.

Sorrentino, A.; Gorrasi, G.; Vittoria, V. (2007). Potential Perspectives of Bionanocomposites for Food Packaging Applications. *Trends in Food Science and Technology*, 18(2), 84-95.

Stoimenov, P. K.; Klinger, R. L.; Marchin, G. L.; Klabunde, K. J. (2002). Metal Oxide Nanoparticles as Bactericidal agents. *Langmuir*, 18, 6679-6686.

Tian, C.; Kaipan, W.; Zhang, Q.; Tian, G.; Zhou, W.; Fu, H. (2010). One Pot Synthesis of Ag Nanoparticles Modified ZnO Microspheres in Ethylene Glycol Medium and their Enhanced Photocatalytic Performance. *Journal of Solid State Chem*istry, 183, 2720-2725.

Unuabonah, E.I., Adewuyi, A., Kolawole, M.O., Omorogie, M.O., Olatunde, O.C., Fayemi, S.O., Günter, C., Okoli, C.P., Agunbiade, F.O., Taubert, A. (2017). Disinfection of Water with New Chitosan-modified Hybrid Clay Composite Adsorbent. *Heliyon* 3(8):
doi: 10.1016/j.heliyon.2017.e00379.

Wang, X. H.; Du, Y. M.; Liu, H. (2004). Preparation, Characterization and Antimicrobial Activity of Chitosan-Zn Complex. *Carbohydrate Polym*er, 56,21-26.

Wang, Y.; Zhang, Q.; Zhang, Ch. L.; Li, P. (2012). Characterization and Cooperative Antimicrobial Properties of Chitosan/Nano-ZnO Composite Nanofibrous Membranes. *Food Chemistry,* 132, 419-427.

Xu, W.; Qim, Z. Y.; Yu, H. Y.; Liu, Y.; Liu, N.; Zhou, Z.; Chen, L. (2013). Cellulolse Nanocrystals as Organic Nanofillers for Transparent Polycarbonate Films. *Journal of Nanoparticle Research,* 15, 1562-1570.

Yang, L.; Mao, J.; Zhang, X.; Xue, T.; Hou, T.; Wang, L.; Tu, M. (2006). Preparation and Characteristics of Ag/nano-ZnO Composite Antimicrobial Agent. *Nanoscience* 11, 44-48.

You, C.; Han, C.; Wang, X.; Zheng, Y.; Li, Q.; Hu, X.; Sun, H. (2012). The Progress of Silver Nanoparticles in the Antibacterial Mechanism, Clinical Application and Cytotoxicity. *Molecular Biology Reports*, 39, 9193-9201.

Yu, H. Y.; Qim, Z. Y.; Liang, B. L.; Liu, N.; Zhou, Z.; Chen, L. (2013). Facile Preparation of Thermally Stable Cellulose Nanocrystals with High Yield of 93% through Hydrochloric Acid Hydrolysis under Hydrothermal Conditions. *Journal of Materials Chemistry A.,* 1, 3938-3944.

Zak, A. K.; Abrishami, M. E.; Majid, W. H.; Yousefi, R.; Hosseini, S. M. (2011). Effect of Annealing Temperature on Some Structural and Optical Properties of ZnO Nanoparticles Prepared by a Modified Sol-Gel Combustion Method. *Ceramics International* 37, 393-398.

Zhou, Q.; Xanthos, M. (2009). Nanosize and Microsize Clay Effects on the Kinetics of the Thermal Degradation of Polylactides. *Polymer Degradation and Stability*, 94, 327-338.

Zhou, S., Zhang, G., Xu, D., Wu, L., Ai, L., Sun, H., Yin, X. (2023). Production and Application of Nanomaterials from Agricultural Waste. In: Neelancherry, R., Gao, B., Wisniewski Jr, A. (eds) Agricultural Waste to Value-Added Products. Springer, Singapore.
doi: 10.1007/978-981-99-4472-9_15